Study of Steel Mass Spring System with varying speeds in the tunnel

Aamir Rashid Chowdhary[*1] and Nasim Akhtar[2, b]

[1]Academy of Scientific and Innovative Research (AcSIR) Ghaziabad-201002, India

[2]CSIR-Central Road Research Institute, New Delhi-110025, India

* Corresponding author, Ph.D. Research Scholar

E-mail: aamirrashid606@gmail.com

[b] Sr. Principal Scientist

E-mail: crri.nasim@gmail.com

Abstract

The Steel Mass Spring System (MSS) has been designed using the Zimmermann method. The impact of speed on the curve radius, cant, stiffness of the MSS, static and dynamic deflection of the MSS is observed and the natural frequency of the MSS is calculated. It has been observed that the speed of the train affects the stiffness of the MSS and therefore the insertion loss. As the speed of the train increases, the characteristic length of the Floating Slab Track decreases due to which the spacing between the MSS also changes and, hence the design of the MSS will be effective.

Keywords: Vibration, Floating Slab Track, Mass Spring System, Natural Frequency, Radius

Introduction

Since railway transportation is energy efficient and generates fewer emissions, it has become increasingly common as a result of global warming. Railway technology has advanced, resulting in increased mobility and convenience as well as an appealing, modern, and environmentally

friendly mode of transportation. The extension of the railway network, on the other hand, has raised environmental concerns. Near railway and transit routes, vibration and noise have a significant effect. In urban areas, mostly the metro lines run under the existing developing units. As such, there are many complaints from the residents regarding the noise and the vibrations generated by the metro operation. The noise and vibration issues are due to the resistance and reverberations over the wheel-rail contact. This vibration adequately transmits through the ground to the neighboring buildings along the line, affecting the residents. The track vibration is caused by the trains running on the track, due to roughness of the wheels, rail corrugation, grinding of wheels and rails, discontinuous rail, and unsmooth track supporting structure. This leads to track vibrations, and these vibrations move through several ways like track system, tunnel structure, geotechnical condition, the foundation of the residential structure, the adjacent buildings. Any vibration above 200 Hz is not considered problematic[1] but is exposed to a low frequency. The most disturbing frequency from the metro is 45-50 Hz. The impact of vibration on humans with high amplitude for a short duration of time can lead to injuries to the muscles or internal organs (< 25 Hz frequency). Vibrations can also lead to malfunctions of sensitive equipment[2,3]. Therefore, measures that are put in place to control the environmental vibrations caused by railway transportation should be both scientific and practical[4-7]. Vibration control can be attained by isolating the source[6], interrupting the vibration path[8] and/or isolating the receiver i.e. the building[9]. There are many vibration control products available worldwide. These include the Vanguard[10], the Cologne Egg[11], the Ladder track[12], Magnetorheological fluids[13], and the Floating slab track[14]. The floating-slab track is the best method to isolate vibration from underground railways[15-17], which can be supported by rubber bearings, glass fiber, polyurethane,

or steel-springs[18]. Normally, two types of mass spring system (MSS) are used in the floating chamber (Table 1):

a) Discrete MSS i.e. Steel MSS and Rubber/Polyurethane MSS

b) Full surface MSS i.e. Polyurethane/Rubber MSS and Rock wool MSS (Density ≥ 350 kg/m^3)

The Floating Slab Track (FST) provides an effective way to reduce the transmission of vibrations from railway traffic to the ground[19-21]. The vibration problems of an FST system have been extensively investigated on the basis of theoretical methods[22-24] and experimental methods[25,26]. The calculation of vibrations generated by moving trains on MSS in underground railway tunnels requires a model that takes into account the dynamics and interaction between the trains, tracks, tunnels, and floors[27]. In addition to the theoretical analysis, some laboratory tests and field tests have also been reported in the literature. The impact of the stiffness and spacing of steel-springs with low-frequency vibration tests was carried out in the track vibration abatement and control laboratory at Beijing Jiao Tong University[28]. The ability to reduce vibration from the steel-spring floating slab track of Beijing metro line 5 in China was tested[29]. On the other hand, the energy transference of the FST system in Singapore was carried out using an analytical method [30].

From the above illustration, it can be seen that many theoretical and experimental research efforts have been dedicated to the dynamic properties of MSS and its impact on ground-borne vibration. However, very few studies have been carried out on the influence of speed and curve radius, which are key technical parameters for MSS design in a tunnel. In Floating Slab Track, there are two stages of concrete in the tunnel. In the first stage, the height varies between 200 mm to 350 mm normally while in the second stage concrete it varies between 225 mm to 600

mm and above. The MSS is installed between the first stage and the second stage of concrete. The gap between the first and the second stage of concrete may vary between 20 mm to 60 mm depending on the availability of the space inside the tunnel. The second stage of concrete plays an important role in controlling the vibration. As the depth of the concrete increases, the natural frequency of MSS decreases accordingly, and thus the attenuation rate increases. In the case of a 5.8 m diameter tunnel, there are two types of electrical power supply to train found in India. One is overhead equipment (OHE) and the other is the third rail. In the case of OHE, on the top of the tunnel system 1m space should be kept and due to the height of the MSS, it requires critical design. Whereas in the case of the third rail, the electrical power supply is on the ground and hence due to the availability of space, the depth of the concrete and space between the first and second stage of concrete can be controlled in the design. The third rail system has been adopted in Kolkata Metro Rail Corporation and Ahmedabad Metro Rail Corporation while the OHE system is in Pune Metro Rail Corporation, Nagpur Metro Rail Corporation, Mumbai Metro Rail Corporation, Chennai Metro Rail Corporation and, Delhi Metro Rail Corporation. Where there is OHE, an increase of height in the second stage of concrete inside a tunnel is a difficult task. Accordingly, the space provided between the first and second stage of concrete is a difficult task for designers. The maximum value of the cant on horizontal curves should also be $1/10^{th}$ to $1/12^{th}$ of the gauge, which should be less than 140 mm[31]. The maximum space for MSS can be 40 mm if the first stage of concrete is less than 250 mm but if the first stage concrete is 300 mm, then it becomes difficult to design the steel MSS due to limited space. This problem can be solved by providing Discrete Polyurethane (PU) Pads MSS or Full Surface Polyurethane MSS with a 20 mm to 30 mm gap. Full Surface Polyurethane MSS is installed in almost all metros in India. However, in terms of vibration control, they are not much effective. Due to this, the Steel MSS,

Discrete PU MSS, and Vanguard system are proposed to be used in other upcoming metros. The metros in India are designed for a speed of 90 kmph while the operating speed is less than 70 kmph because the station to station distance is around one kilometer. It has been measured that less vibrations are generated in the straight portion while on the curved portion vibration increases drastically (Delhi metro). Normally, in the straight portion operating speed varies between 60-70 kmph while on the curve portion (radius <450 m), it is around 50 kmph or less. In this paper, the authors have taken a typical 5.8 m diameter tunnel and designed steel MSS with different varying conditions like speed, radius, and cant. Different types of MSS specifications as per DIN EN 13906-1: 2013-11[32] have been used for fatigue tests for the design of MSS. This paper provides the results of the study for the steel MSS based on different parameters like FST material parameters[33], rolling stock parameters[34], track parameters, and elastic support parameters[32].

The evaluation of steel MSS by Zimmermann Method

In this paper, the Zimmermann method is used for static and dynamic analysis for the MSS design, calculation of vertical natural frequency, stiffness of MSS, fatigue verification, and calculation of insertion loss based on vertical natural frequency and damping ratio (Spectral analysis in the third-octave band).

Spring unit used in this design

There are two types of springs in a housing; external spring and internal spring. The diameter of the external spring is 44 mm and the total number of turns is 03, while in the case of the internal spring the diameter is 20 mm and the total number of turns is 5.6. Modulus of Elasticity, E =

206000 N/mm^2 and Shear Modulus, G= 78500 N/mm^2. The height of the block is less than 185 mm.

The Vertical spring rate (k_v) and Horizontal spring rate(k_H) is expressed as:

$$k_v = G\frac{d^4}{8nD^3} \quad (1)$$

$$k_{H\ \text{static + dyn}} = \eta_{\text{static + dyn}}.k_v \quad (2)$$

Where G is shear modulus, d is the diameter of spring, n is the number of turns, D is spring housing diameter, η is the ratio horizontal to the vertical spring rate.

To calculate the fatigue strength of the MSS, the stresses in the external and internal springs on the outside and inside track is calculated as:

Maximum vertical spring load,

$$V_{\text{static+dyn } MAX} = Gd^4 d_{\text{static+dyn } MAX}/8nD^3 \quad (3)$$

Maximum horizontal spring load,

$$H_{\text{static+dyn } MAX} = k_{H\ \text{static+dyn}}\, d_{\text{static+dyn } HOR} \quad (4)$$

Where, $d_{\text{static + dyn VER}}$ is vertical deflection,

$d_{\text{static + dyn HOR}}$is horizontal deflection

Rail Type- UIC 60[35]

The UIC 60 rail has been used having a modulus of elasticity of rails, E_{RAIL}= 2.10E+08 kN/m², rail height, h_{RAIL}=172 mm, the second moment of area of rails, I_{RAIL}=3055 cm^4, area of the cross-section of the rails, A_{RAIL} =76.87 cm², mass per linear meter of rail, μ_{RAIL}=60.34 kg/m, the center of gravity, z_{CG} =80.9 mm and mass per linear meter of the fasteners, μ_{FAST} =92.3 kg/m.

FST Cross-Section Properties

The cross-section of the tunnel with dia 5.8 m, UIC 60 Rail, stage II and stage I concrete as well as steel MSS has been shown in Figure 1 while the FST cross-section has been shown in Figure 2.

For designing the steel MSS, the following equations have been used:

$$\text{Cant,} \quad s = bit.v^2/gR \tag{5}$$

Where bit = gauge length

v= speed of the train

g= acceleration due to gravity

R= curve radius

The cross-sectional area, CoG, and linear mass of the FST are calculated for determining the vertical natural frequency of the MSS as:

Cross-sectional area of the FST, $A_{conc\ transv} = bh + 2(h_1 b_1) + h_1 b_2 + 2(hb_3)/2$ (6)

CoG of the track bed,

$$CoG_{FST} = (A_{con\ transv}\delta_{conc} CoG_{slab} + 2A_{rail}\delta_{steal}(h + h_1 + z_{CG})) / (A\delta_{conc} + 2A_1\delta_{conc} + 2A_{rail}\delta_{steal}) \tag{7}$$

Linear Mass of the FST, $\mu_{FST} = A_{conc\ transv}\delta_{conc} + 2\mu_{Rail} + \mu_{FAST}$ (8)

Using equations (6), (7), and (8), 2nd moment of area of the FST is calculated as:

$$Iy_{FST} = [bh^3/12 + bh(CoG_{FST} - h/2)^2 + [2(b_1 {h_1}^3/12 + b_1 h_1 (CoG_{FST} - h_1/2)^2)] + [(b_2 {h_1}^3/12 + b_2 h_1 (CoG_{FST} - h_1/2)^2)] + [2(b_3 h^3/36 + b_3 h(CoG_{FST} - h/2)^2)] + [2(I_{RAIL} + A_{RAIL}(CoG_{FST} - (h + z_{CG})^2)] \tag{9}$$

Also, the modulus of rigidity of the FST is calculated as:

$$EI_{FST} = E_{conc}(I_{CoG} + I_{1_{CoG}}) + E_{RAIL}I_{RAIL_{CoG}} \quad (10)$$

FST Stiffness

The stiffness of the FST depends on the spring rate and longitudinal spacing outside and inside of the curve and has been calculated using equations (11) to (16) as:

Vertical stiffness per m length of outside FST, $k_{v_{FST_{out}}} = k_v / spac_{long_{out}}$ (11)

Vertical stiffness per m length of inside FST, $k_{v_{FST_{in}}} = k_v / spac_{long_{in}}$ (12)

Horizontal stiffness per m length of outside FST, $k_{H_{FST_{out}}} = k_H / spac_{long_{out}}$ (13)

Horizontal stiffness per m length of inside FST, $k_{H_{FST_{in}}} = k_H / spac_{long_{in}}$ (14)

Using equations (11)-(14), the vertical and horizontal stiffness per m length of FST is calculated as:

Vertical stiffness per m length of FST, $k_{v_{FST}} = k_v / spac_{long_{out}} + k_v / spac_{long_{in}}$ (15)

Horizontal stiffness per m length of FST, $k_{H_{FST}} = k_H / spac_{long_{out}} + k_H / spac_{long_{in}}$ (16)

Where $spac_{long_{out}}$ is longitudinal spacing outside of the curve

$spac_{long_{in}}$ is longitudinal spacing inside of the curve

k_v is vertical spring rate

k_H is horizontal spring rate

Load combinations to calculate the natural frequency and fatigue verification

The results of static load and centrifugal force caused by train operation are calculated using equations (17) and (18) as:

Static load (FST Weight), $F_{FST} = \mu . g$ (17)

Centrifugal force, $F_{centr} = (F_{vert\ axle} / g)(v^2 / R)$ (18)

Resultant load to calculate the natural frequency

To calculate the natural frequency, the resultant vertical load outside and inside the wheel is calculated using equations (19) and (20) as:

Resultant vertical load outside wheel for v = 30,50,70,80 and 90 kmph

$$F_{res_{V_{out}}} = (F_{vert_V} + F_{centr_V})/2 + [(h + h_1 + h_{RAIL} + cog)/spac_{TRANSV}](F_{centr_H} - F_{vert_V}) \quad (19)$$

Where $spac_{TRANSV}$ is transverse spacing between spring units= 2 m

Resultant vertical load inside wheel for v = 30,50,70,80 and 90 kmph

$$F_{res_{V_{in}}} = (F_{vert_V} + F_{centr_V})/2 - [(h + h_1 + h_{RAIL} + cog)/spac_{TRANSV}](F_{centr_H} - F_{vert_V}) \quad (20)$$

Using equations (10) and (15), the characteristic length of the FST is calculated as

$$L_{charact} = (4EI_{FST} / k_{v_{FST}})^{1/4} \quad (21)$$

Where $k_{v_{FST}}$is stiffness (Spring rate) per meter= modulus of subgrade x width of the FST

FST dynamic vertical deflections

The speed of the train directly effects the dynamic vertical deflections both outside and inside of the wheel and using equations (22) and (23), the maximum dynamic deflection for determining the fatigue and clearance is calculated as:

Dynamic deflection outside, $d_{dyn_{out}}(x) = \Sigma_i = 1\ldots12\ [d_i(x)\, w_{i_{out}}]$ (22)

Dynamic deflection inside,$d_{dyn_{in}}(x) = \Sigma_i = 1\ldots12\ [d_i(x)\, w_{i_{in}}]$ (23)

Maximum dynamic deflection outside wheel for determining fatigue &clearance for v = 30,50,70,80 and 90 kmph

$$d_{dyn_{out_{fat}}} = MAX\,[\,d_{dyn_{out}}(x)\,] \qquad (24)$$

Maximum dynamic deflection inside wheel for determining fatigue &clearance for v = 30,50,70,80 and 90 kmph

$$d_{dyn_{in_{fat}}} = MAX\,[\,d_{dyn_{in}}(x)\,] \qquad (25)$$

FST static vertical deflections

Using equations (15) and (16), the static vertical deflections outside and inside of the wheel is calculated as:

Static deflection, $d_{static} = F_{static} / k_{v_{FST}}$ (26)

Static deflection - outside, $d_{static\ out} = F_{static\ out} / k_{v_{FST\ out}}$ (27)

Static deflection - inside, $d_{static\ in} = F_{static\ in} / k_{v_{FST\ in}}$ (28)

FST dynamic horizontal deflection

To calculate the dynamic horizontal deflections outside and inside of the wheel, the horizontal component of traffic load on track, the load distribution between the axles in adjacent bogies should be considered, and by using equation (16), the maximum dynamic horizontal deflection for v =30,50,70,80 and 90 kmph is calculated as:

$$d_{\ dyn\ HOR\ fn} = (F_{centr\ H} - F_{vert\ H})12\ axles / ((x_{\ axle\ 12} - x_{\ axle\ 1})\, k_{H_{FST}}) \qquad (29)$$

Using equation (16) and taking the effect of the transverse load outside the wheel, maximum dynamic horizontal deflection is determined for fatigue & clearance as:

$$d_{dyn\,HOR\,fat} = F_{res\,H\,out}\,12\ axles\ /\ (\,(\,x_{axle\,12} - x_{axle\,1}\,)\,k_{H_{FST}} \qquad (30)$$

FST static horizontal deflection

Using equations (16) and (17), the static horizontal deflections outside and inside of the wheel is calculated as:

$$d_{static\,HOR} = F_{est}\,sen\,\theta\ /\ k_{HLF} \qquad (31)$$

FST vertical natural frequency

Using equations (24), (25), (26), and by considering the unsprung train mass, the vertical natural frequency of the FST is calculated as:

$$f_{n\,train} = 5\ /\ [\,(\,(\,(\,d_{dyn\,OUT\,fn} + d_{dyn\,IN\,fn}\,)\ /\ 2\,)m_{train\,fn} + d_{static})\ /\ 10\,]^{\frac{1}{2}} \qquad (32)$$

The calculation of insertion loss based on vertical natural frequency and damping ratio of the Mass Spring System (Spectral analysis in third-octave bands) depends on the transmissibility (T) which is expressed as:

$$T = [\,(\,1 + 4D^2\eta^2\,)\ /\ (\,(1 - \eta^2)24D^2\eta^2\,)\,]^{0.5} \qquad (33)$$

Where η= Tuning ratio

D = Damping ratio related to critical damping

Results and Discussion

The static and dynamic responses and the natural frequency of the Steel MSS are calculated based on the Influence lines **(**Zimmermann Method). The design parameters of the MSS are listed in Table 2. In this study for a speed range from 30 kmph to 90 kmph, the diameter of the tunnel has been taken as 5.8 m. This study shows that as the speed of the train increases, the required cant will also increase. Therefore, to design an economical section, the longitudinal spacing and radius of the curve must be adjusted accordingly. Also, the fatigue verification of the steel MSS is to be done and it should be under the permissible limit.

Impact of speed on the curve radius and cant

The safest design for different speeds/ radius/cant has been made. If the curve radius is 200 m then it will be difficult to run the train at a speed above 30 kmph. Therefore, the practical design has been suggested in this study with varying train operating speed, curve radius, and actual site conditions. In this study, the 30 kmph to 90 kmph speed of the train has been taken with a varying radius from 200 m to 660 m as shown in Table 3. It is observed that as the speed of the train and curve radius increases, the cant will also increase which is 50.79 mm at 30 kmph and 138.52 mm at 90 kmph which is found to be under the permissible limit. The most critical section began where the radius of the tunnel is less than 350 m, at this radius, the vibration attenuation becomes a major problem due to interaction between rail and wheel, here the speed plays a minor role.

Static and dynamic responses of MSS

Vertical static and dynamic deflection play an important role while designing the MSS. There are two types of dynamic deflection, namely dynamic deflection outside track and inside track (Figures 3, 5 & 6). As the speed of the train increases from 30 kmph to 90 kmph, the maximum dynamic deflection outside the track decreases from 5.83 mm to 5.69 mm. The maximum dynamic deflection for the inside track starts decreasing with the increase in speed i.e. 4.98 mm to 3.87 mm. The reason for this declining trend of dynamic deflection is that with the increase in the train speed, the static effect of the load decreases. It is observed that the static deflection outside track and the inside track is in a decreasing trend i.e. 4.23 mm at 30 kmph and 3.83 mm at 90 kmph (Table 3). Steel MSS used in this study has been designed for 9.71 mm which is the permissible dynamic deflection amplitude. It is observed that the maximum deflection for the design proposed in this paper is under the permissible limit being 5.83 mm on the outside track and 4.98 mm on the inside track.

For fatigue verification, the static and dynamic stresses in the internal and external springs are also under permissible limits according to Goodman Diagram DIN EN 13906-1-2013-11 (Figures 4(a & b) and 7 (a & b)). For internal spring, at 0 N/mm^2 the permissible static and dynamic stress is found to be 508 N/mm^2 and at 425 N/mm^2 it is 804 N/mm^2 but after 425 N/mm^2 begins to behave linearly. Similarly for the external spring, at 0 N/mm^2 the permissible static and dynamic stress is found to be 357 N/mm^2 and at 485 N/mm^2 it is 709 N/mm^2 but after 485 N/mm^2 it begins to behave linearly.

The vertical spring rate in the external and internal spring is constant at each speed, but the horizontal spring rate for the external spring is 4500.38 N/mm at 30 kmph and reaches up to 4499.39 N/mm at 90 kmph (Figure 8(a)) and the horizontal spring rate for internal spring is

426.67 N/mm at 30 kmph and decreases with increase in the speed increases i.e. at 90 kmph its value is 427.62 N/mm (Figure 09(b)).

Vertical natural frequency of MSS

The natural frequency of the steel MSS has been observed to vary between 7.04 Hz and 7.40 Hz (Table 3). It shows that the attenuation should start after 9.95 Hz and 10.46 Hz and attenuate up to 26-28 VdB, which is found to be a good amount of vibration attenuation at source for Steel MSS as per RDSO. The vibration attenuation with and without the application of steel MSS has been shown in Figures 9 and 10 for varying speeds. The vibration level in the tunnel, before application of the steel MSS was 90 VdB at 80 Hz, which is well above the permissible limit of 72 VdB (RDSO). However, after the application of steel MSS, vibration attenuation has been observed; at 80Hz the maximum vibration attenuation of 35.8 VdB takes place at each speed, which is much more than the global attenuation value of 27.5 VdB at 30 kmph, 27.2 VdB at 50 kmph, 27.1 VdB at 70 kmph, 27 VdB at 80 kmph and 26.8 VdB at 90 kmph. The emission from the tunnel floor remains constant at each speed; at 32 VdB at 4 Hz and it is 56 VdB at 80 Hz.

The results given in Table 3, show that when the train speed increases from 30 kmph to 90 kmph, the characteristic length of the FST and the longitudinal spacing between the MSS shows a decreasing trend. The resulting load for calculating the natural frequency and for the verification of the tunnel clearance and the fatigue verification for the outside wheel increases with the train speed. It is 86.61 KN at 30 kmph and 98.03 KN at 90 kmph. The resulting vertical load for the inside wheel decreases with increasing speed; 73.39 KN at 30 kmph and 61.97 KN at 90 kmph. It is also observed that the vertical stiffness per meter length of the FST of the single trackbed is 8.55 KN/mm at 30 kmph and 9 KN/mm at 90 kmph while the horizontal stiffness per meter

length of the FST of the single trackbed is 6.36 KN/mm at 30 kmph and 6.88 KN/mm at 90 kmph. As the natural frequency depends on the stiffness of the MSS, it should always be less for higher vibration attenuation

Conclusion

In this paper, the static and dynamic analysis of the steel MSS is performed using the Zimmermann method, and the influence of the speed, radius, and cant on the steel MSS is observed. The following conclusions are drawn from this study:

- As the speed of the train increases, the dynamic deflection both outside and inside wheel decreases. The maximum dynamic deflection of 5.83 mm is under the permissible limit and it has a major effect on the design of MSS.
- As the speed of the train increases, so does the curve radius, which ultimately decreases the characteristic length of the FST and thus changes the longitudinal spacing between the MSS thereby lowering the cost and thus making the design economical.
- For a cost-effective design, in the curve section, steel MSS should be provided for a length of 150 m on both sides from the centre of the curve while on the straight section, discrete PU MSS is to be adopted.
- The insertion loss (vibration attenuation) depends on the natural frequency of the steel MSS, the lower the natural frequency, the greater will be the insertion loss, and vice-versa. As the speed of the train increases, the stiffness of the MSS also increases, leading to an increase in the natural frequency of MSS, which directly affects the vibration attenuation of the steel MSS.

- All results have been verified with the fatigue test and correspond to the Goodman Diagram.

Declaration of Conflicting Interests

The author(s) declare that there is no conflict of interests with respect to the publication of this article.

ACKNOWLEDGEMENT

We thank the AcSIR-CRRI, New Delhi, and the Transport Planning & Environment Division, CSIR-Central Road Research Institute, New Delhi for their help and collaboration in this study.

References

1. Jones, C.J.C. and Block J.R., Prediction of ground vibration from freight trains. Journal of Sound and Vibration, 1996, Vol. 193, Issue 1, pp. 205-213.
2. Gordon, C.G., Generic vibration criteria for vibration-sensitive equipment. Proceedings of SPIE, 1999, pp. 22-39.
3. ISO-2631 Part-1., Mechanical vibration and shock- Evaluation of human exposure to whole-body Vibration - Part 1: General Requirements, 1997.
4. Volberg, G., Propagation of ground vibrations near railway tracks. Journal of Sound and Vibration,1983, Vol. 87, Issue 2, pp. 371-376.
5. Bata, M., Effects on buildings of vibrations caused by traffic. Building Science, 1985, Vol. 99, Issue 1, pp. 1-12.
6. Wilson, G. P., Saurenman, H. J. and Nelson, J. T., Control of ground-borne noise and vibration, Journal of Sound and Vibration, 1983, Vol.87, Issue 2, pp. 339-350.

7. Xue, Y., Li, S., Zhang, D., Sun, X., Sun, Z., Nie, Y., Vibration characteristics and environmental responses of different vehicle-track-ballast coupling systems in subway operation, Journal of Vibroengineering, 2014, Vol. 16, Issue 5, pp. 2458-2473.
8. Woods, R. D., Screening of surface waves in soils, Journal of the Soil Mechanics and Foundations Division ASCE, 1968, pp. 951-979.
9. Talbot, J. P. and Hunt, H.E.M., On the performance of base-isolated buildings, Building Acoustics, 2000, Vol.7, Issue 3, pp. 163-178.
10. Cox, S. J., Wang A., Morison C., Carels P., Kelly R., Bewes O. G., A test rig to investigate slab track structures for controlling ground vibration. Journal of Sound and Vibration, 2006, Vol. 293, Issues 3-5, pp. 901-909.
11. Zhou, M., Wei K., Zhou S., Xiao J., Gong Q., Influence of different track types on the vibration response of the jointly-built structure of subway and the buildings. China Railway Science, 2011, Vol. 32, Issue 2, pp. 33-40.
12. Yan, Z. Q., Markine V., Gu A. J., Liang Q. H., Optimization of the dynamic properties of ladder track to control rail vibration using the multipoint approximation method. Journal of Vibration and Control, 2014, Vol. 20, Issue 13, pp. 1967-1984.
13. Raju, R. K., and Vineeth, V. D., Developments in vibration control of structures and structural components with magnetorheological fluids, Current Science, 2017, Vol. 112, No. 3, pp. 499-508.
14. Lopes, P., Costa P. A., Calcada R., Cardoso A. S., Mitigation of vibrations induced by railway traffic in tunnels through floating slab systems: numerical study. Eurodyn 2014: 10th International Conference on Structural Dynamics, 2014, pp. 871-878.

15. Grootenhuis, P., Floating track slab isolation for railways. Journal of Sound and Vibration, 1977, Vol. 51, Issue 3, pp. 443-448.
16. Nelson, J. T., Recent developments in ground-borne noise and vibration control. Journal of Sound and Vibration, 1996, Vol. 193, Issue 1, pp. 367-376.
17. Kurzweil, L.G., Ground-borne noise and vibration from underground rail systems. Journal of Sound and Vibration, 1979, Vol. 66, no. 3, pp. 363–370.
18. Hussein, F.M. and Hunt, E., Modelling of Floating-Slab Track with Discontinuous Slab .Part 1: Response to Oscillating Moving Loads, Journal of Low Frequency Noise Vibration and Active Control , 2006, pp.23-39.
19. Lombaert, G., Degrande, G., Vanhauwere, B., Vandeboght, B., and Francois, S., The control of ground-borne vibrations from railway traffic by means of continuous floating slabs, Journal of Sound and Vibration, 2006, pp. 946–96.
20. Hussein, M. F. M. and Hunt, H. E. M., Modelling of floating-slab tracks with continuous slabs under oscillating moving loads. Journal of Sound and Vibration, 2006, pp.37-54.
21. Kuo, C., Huang, C., and Chen. Y., Vibration characteristics of floating slab track. Journal of Sound and Vibration, 2008, pp.1017-1034.
22. Zhou, B., Xie, X.Y. and Yang, Y.B., Simulation of wave propagation of floating slab track-tunnel-soil system by 2D theoretical model. International Journal of Structural Stability and Dynamics, 2014,Vol.14, pp. 1-24.
23. Connolly, D.P., Kouroussis, G., Laghrouche, O., Ho, C.L., Forde, M.C., Benchmarking railway vibrations—track, vehicle, ground and building effects. Construction and Building Materials, 2015, Vol. 92, pp. 64–81.

24. Lei, X .Y. and Jiang C.D., Analysis of vibration reduction effect of steel spring floating slab track with finite elements. Journal of Vibration Control, 2016, Vol.22, pp.1462–1471.
25. Ding, D.Y., Liu, W.N., Li, K.F., Sun, X.J., Liu, W.F., Low frequency vibration tests on a floating slab track in an underground laboratory. Journal of Zhejiang University-SCIENCE A (Applied Physics & Engineering), 2011, Vol.12, pp. 345–359.
26. Zhu, S., Wang, J., Cai, C., Wang, K., Zhai, W., Development of a vibration attenuation track at low frequencies for urban rail transit. Computer-Aided Civil and Infrastructure Engineering, 2017,Vol. 32, pp.713–726.
27. Hussein, M. F. M., A comparison between the performance of Floating Slab Tracks with continuous and discontinuous slabs in reducing vibration from underground railway tunnels, 16th International Congress on Sound and Vibration Karakow, Poland, 2009, pp. 46-51.
28. Liu, W., Ding, D., Li, K., and H. Zhang., Experimental study of the low-frequency vibration characteristics of steel spring floating slab track, Tumu Gongcheng Xuebao/China Civil Engineering Journal, 2011,Vol.44, pp.118–125.
29. Li, K., Liu, W., Sun, X., Ding, D., and Yuan. Y., In-site test of vibration attenuation of underground line of Beijing metro line 5, Journal of the China Railway Society, 2011, Vol.33, pp.112–118.
30. Cui, F. and Chew, C.H., The effectiveness of floating slab track system-Part I. Receptance methods. Appl Acoust, 2000,Vol.61, pp. 441–453.
31. Chandra, S. and Agarwal, M.M., Railway Engineering, Oxford University Press, New Delhi, 2007.

32. DIN EN 13906-1: Cylindrical helical springs made from round wire and bar-Calculation and design- Part-1: Compression springs, 2013-11.
33. IS 456: Plain and Reinforced Concrete- Code of Practice, 2000.
34. Bombardier Movia Metro for New Delhi.
35. BS EN 13674-1., Railway applications - Track - Rail - Part 1: Vignole railway rails 46 kg/m and above (includes Amendment A1), 2017.
36. Michael, S., Standards and Tests of Fastening Systems. Conference and Proceeding. AREMA Annual Conference presentation Chicago- Illinois, 2007.
37. Kurrer, K.E., A History of the Theory of Structures: from Arch Analysis to Computational Mechanics. Berlin: Ernst &Sohn Verlag für Architektur und technische Wissenschaften GmbH & Co.KG. Berlin, 2008.
38. Prakoso, P. B., The Basic Concepts of Modelling Railway Track Systems using Conventional and Finite Element Methods Info Teknik, 2012, Vol. 13, pp. 57-65.
39. Research Design and Standards Organization (RDSO)-ISO-9001, Ministry of Railways, Govt. of India.
40. Federal Transit Administration (FTA), U.S. Department of Transportation.

Table 1. Different Types of Mass Spring System[39,40]

MSS	Steel MSS	PUR-Discrete MSS	PUR-Full Surface MSS
Natural frequency (Hz)	7-8	12-14	20
Attenuation start (Hz)	10-11	20	28.28
Global value killing (VdB)	26-28	15-17	9.6

Table 2. Steel MSS Design Parameters

Diameter(m)	5.8
Maximum Axle Load (KN)	160
Minimum Axle Load (KN)	85
Rail type	UIC60
Critical damping ratio	8%
Dynamic factor / Overload Factor	1.49
Width of the Floating Slab Track, b (m)	2.758
Width of the side beams, b_1 (m)	0.387
Width of the central beam, b_2 (m)	1.000
Width of the side triangles, b_3 (m)	0.487
Height of FST without beams, h (m)	0.338
Height of the longitudinal beams, h_1(m)	0.122
CoG of Slab, CoG (m)	0.214
Braking load - 12.5% of the vertical axle load (KN)	20
Length of Wagon, C_{wag}(m)	25
Height of Wagon, h_{wag}(m)	4.048
Width of Wagon, b_{wag}(m)	3.20
Number of axles, n_{axles}	12
Axle spacing in the same bogie(m)	2.5
Unsprung train mass (part of the train mass oscillating at same DoF as our track slab)	15%
Vertical spring stiffness, k_v (KN/mm)	6.63

Horizontal spring stiffness, k_H (KN/mm)	4.93
Static Load - FST Weight (KN per meter single track)	36.23

Table 3. Design Calculations for Steel Mass Spring System

Speed (Kmph)	30	50	70	80	90
Characteristic length of the FST (m)	4.33	4.26	4.23	4.23	4.23
Radius (m)	200	280	400	520	660
Cant(mm)	50.79	100.77	138.26	138.92	138.52
Longitudinal spacing (m)	1.55	1.45	1.41	1.405	1.4
Centrifugal force (KN / axle)	5.56	11.02	15.12	15.19	15.15
Resultant vertical load outside wheel (KN)	86.61	93.12	97.99	98.08	98.03
Resultant vertical load inside wheel (KN)	73.39	66.89	62.01	61.92	61.97
Static deflection - inside (mm)	4.23	3.96	3.85	3.84	3.83
Static deflection - outside (mm)	4.23	3.96	3.85	3.84	3.83
Vertical stiffness per m length of FST (KN/mm)	8.55	8.70	9.40	8.97	9.00
Horizontal stiffness per m length of FST (KN/mm)	6.36	6.65	6.99	6.86	6.88

Figure 1. Typical Cross Section of steel MSS inside tunnel having dia 5.8 m

Figure 2. Floating Slab Track Cross-Section

Figure 3. Vertical static and dynamic deflection of MSS at 30 kmph speed

Figure 4 (a). Stresses in the external springs on the outside and inside track at 30 kmph speed

Figure 4 (b). Stresses in the internal springs on the outside and inside track at 30 kmph speed

Figure 5. Change in dynamic deflection in the inside track with respect to 30 kmph speed

Figure 6. Change in dynamic deflection in the outside track in comparison to 30 kmph speed

Figure 7 (a). Stresses in the external springs on the outside and inside track

Figure 7 (b). Stresses in the internal springs on the outside and inside track

Figure 8(a). Static and dynamic horizontal spring rate

Figure 8(b). Static and dynamic horizontal spring rate

Figure 9. Vibration levels with and without MSS at 30 kmph speed

Figure 10. Vibration levels with and without MSS with respect to 30 kmph speed

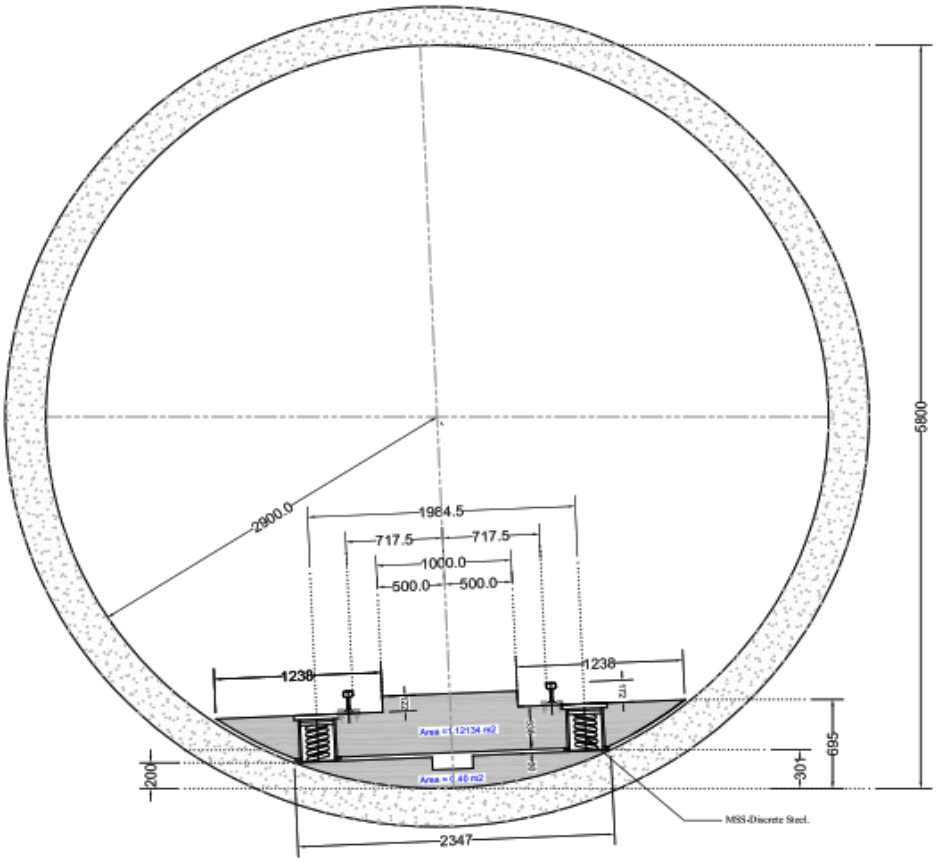

Figure 1. Typical Cross Section of steel MSS inside tunnel having dia 5.8 m

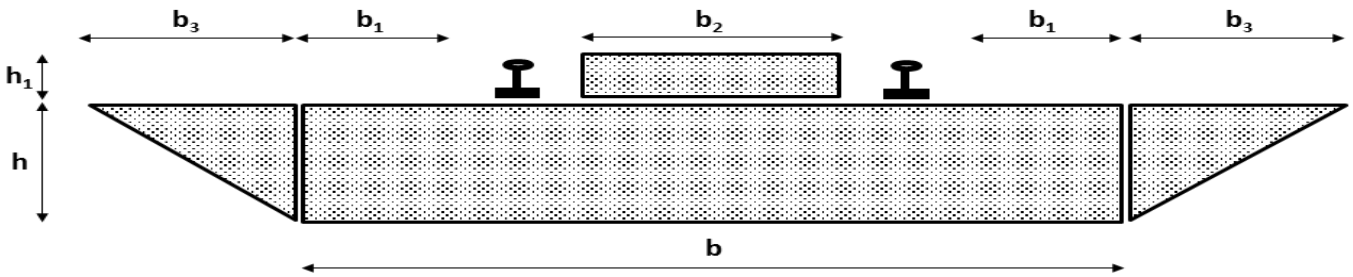

Figure 2. Floating Slab Track Cross-Section

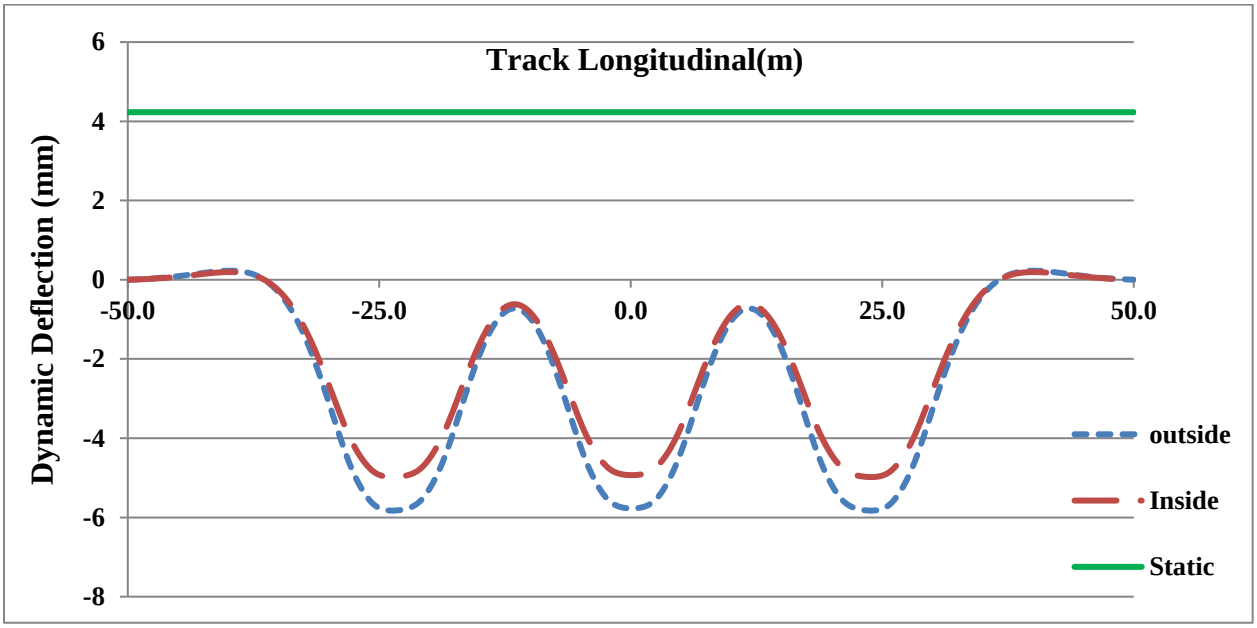

Figure 3. Vertical static and dynamic deflection of MSS at 30 kmph speed

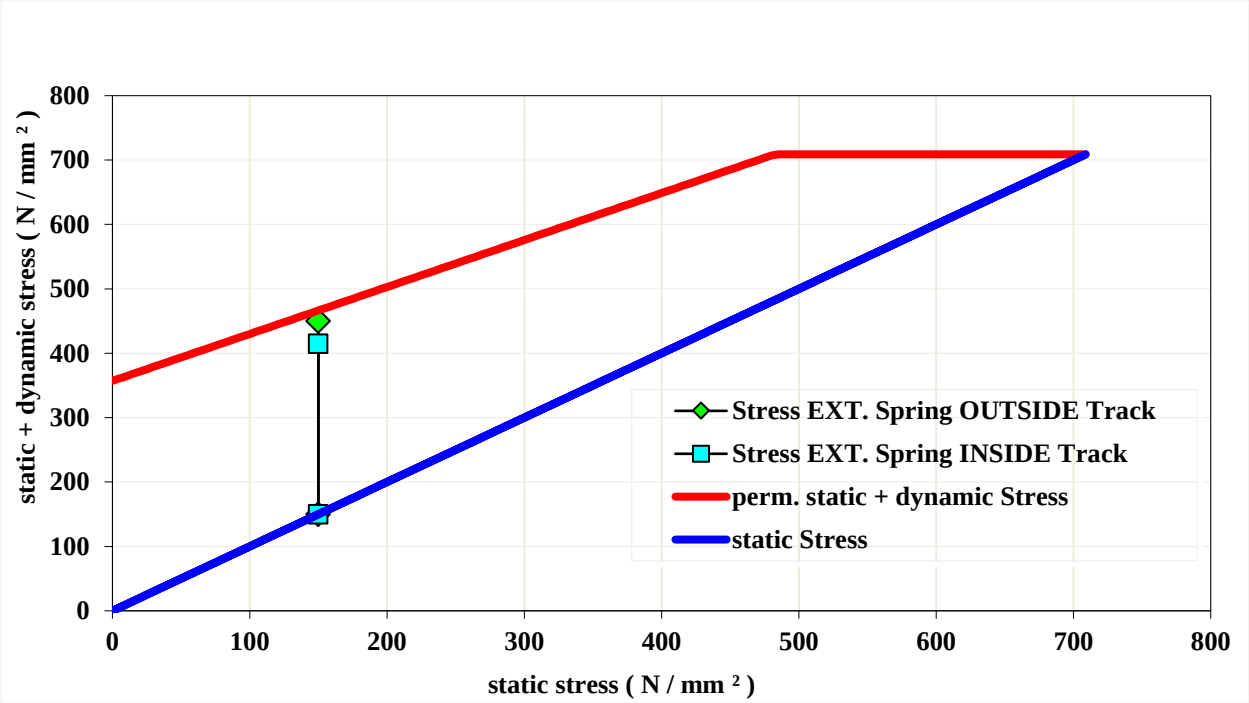

Figure 4 (a). Stresses in the external springs on the outside and inside track at 30 kmph speed

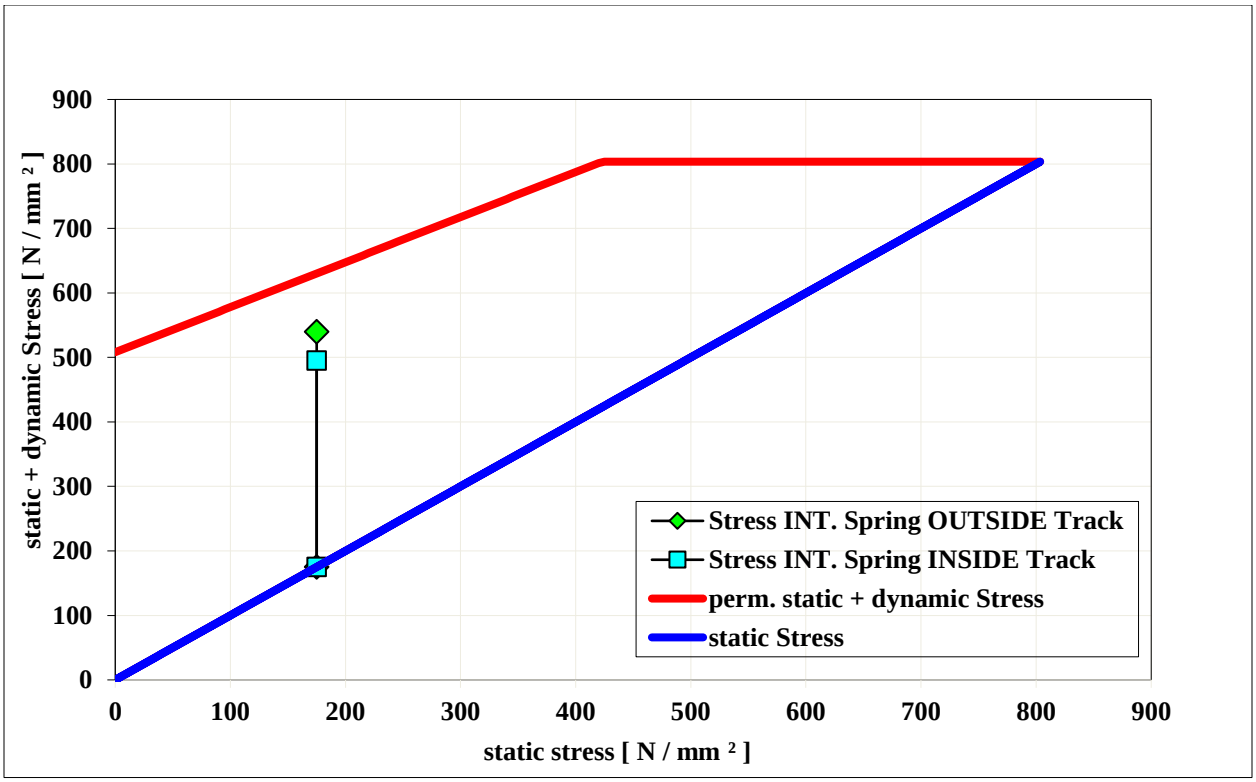

Figure 4 (b). Stresses in the internal springs on the outside and inside track at 30 kmph speed

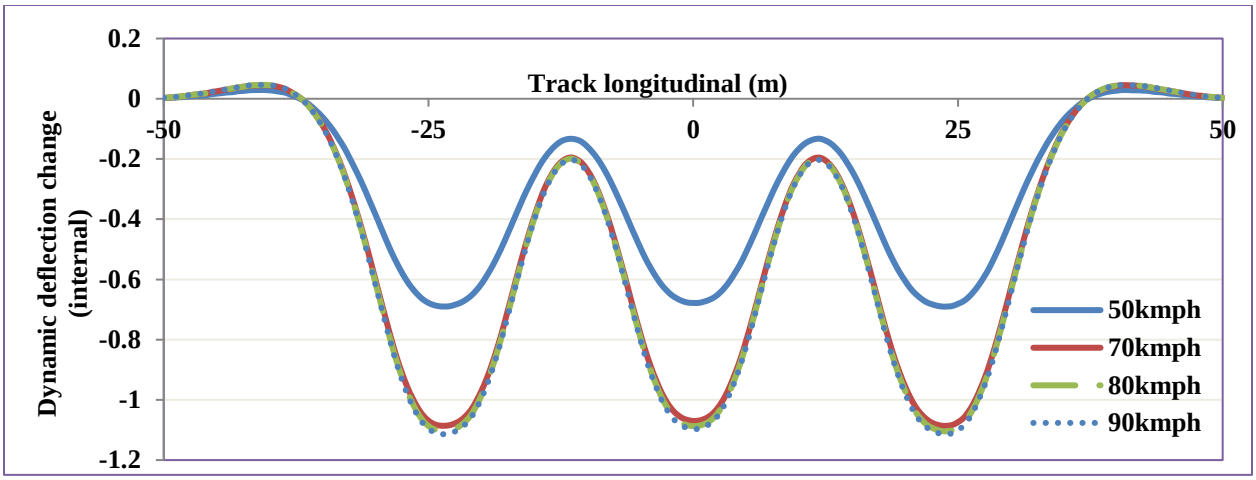

Figure 5. Change in dynamic deflection in the inside track with respect to 30 kmph speed

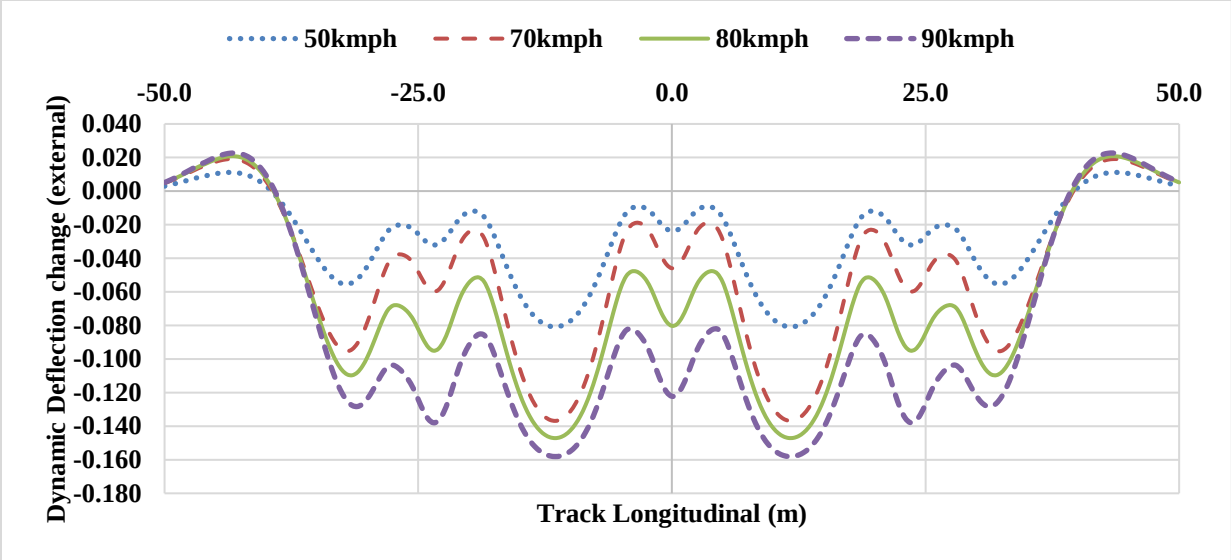

Figure 6. Change in dynamic deflection in the outside track in comparison to 30 kmph speed

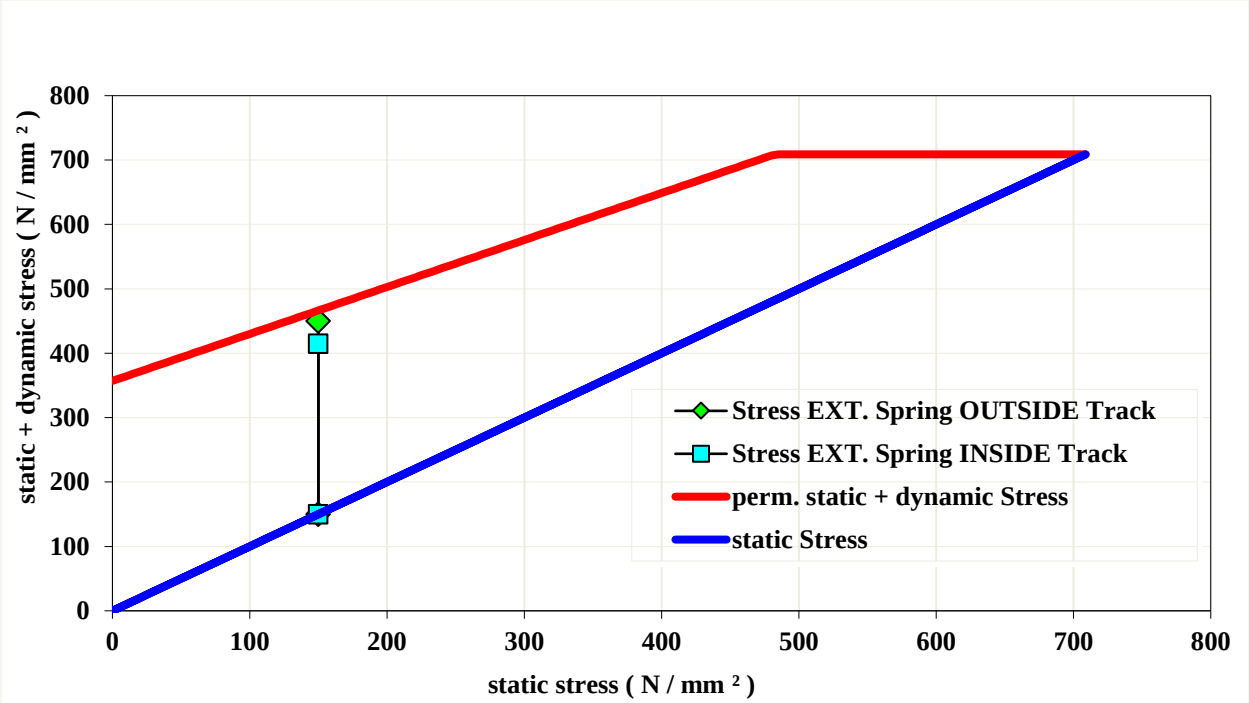

Figure 7 (a). Stresses in the external springs on the outside and inside track

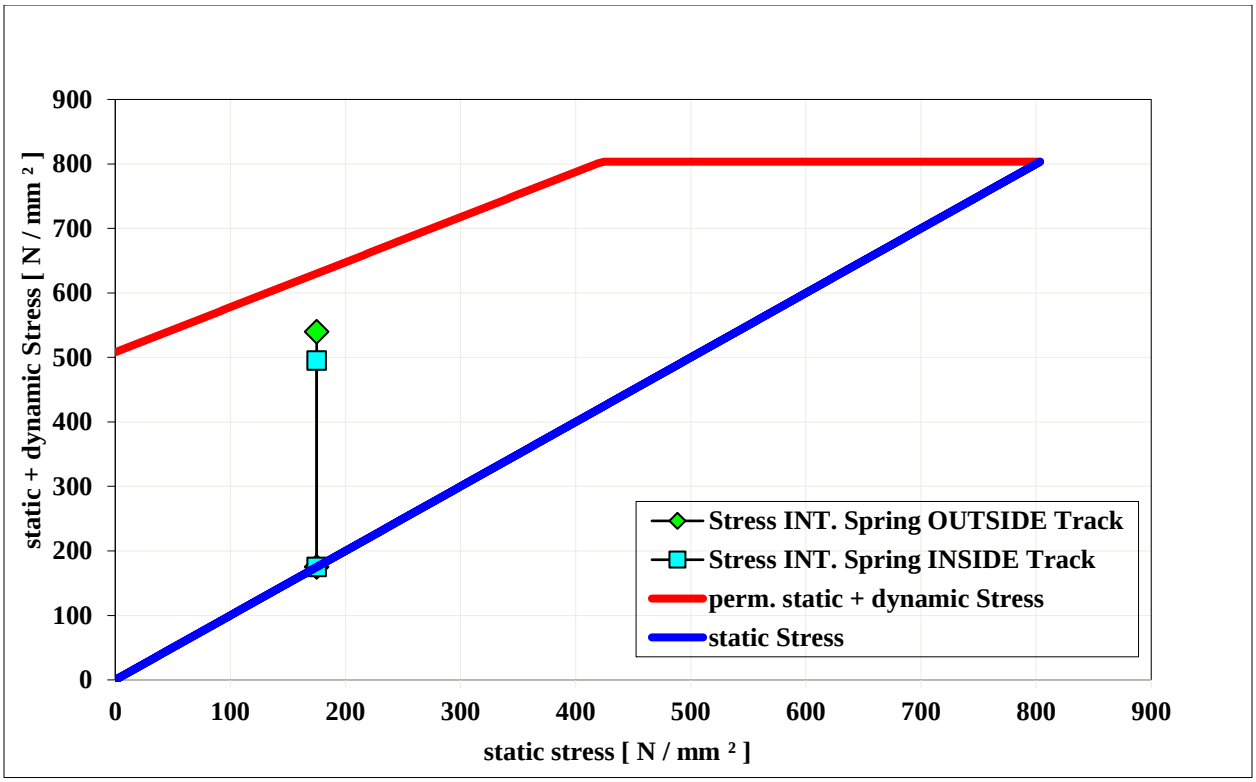

Figure 7 (b). Stresses in the internal springs on the outside and inside track

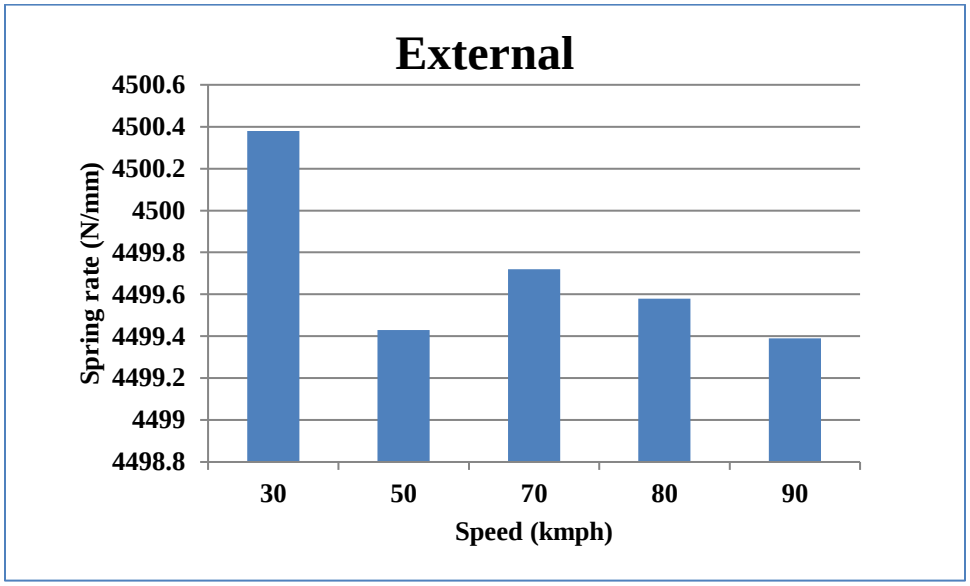

Figure 8(a). Static and dynamic horizontal spring rate

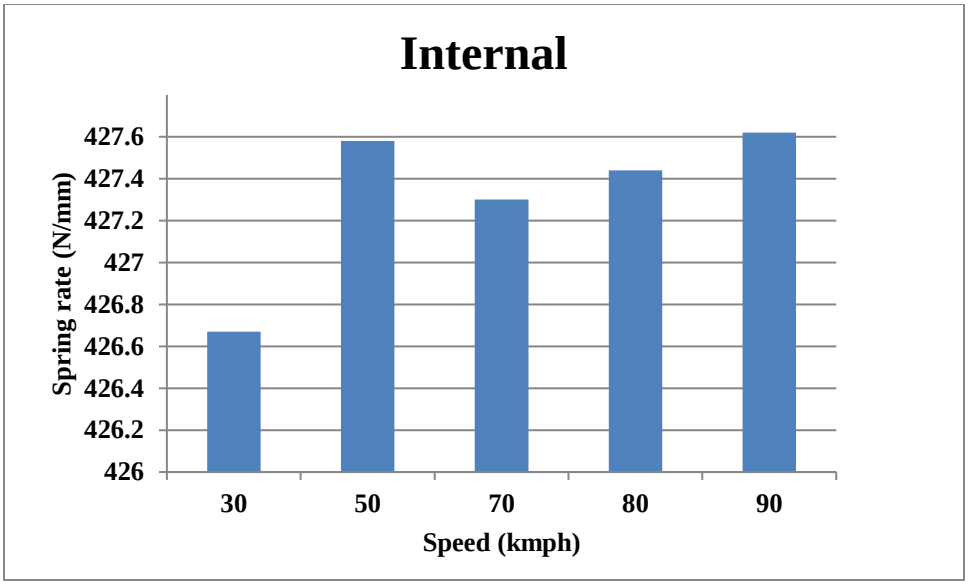

Figure 8(b). Static and dynamic horizontal spring rate

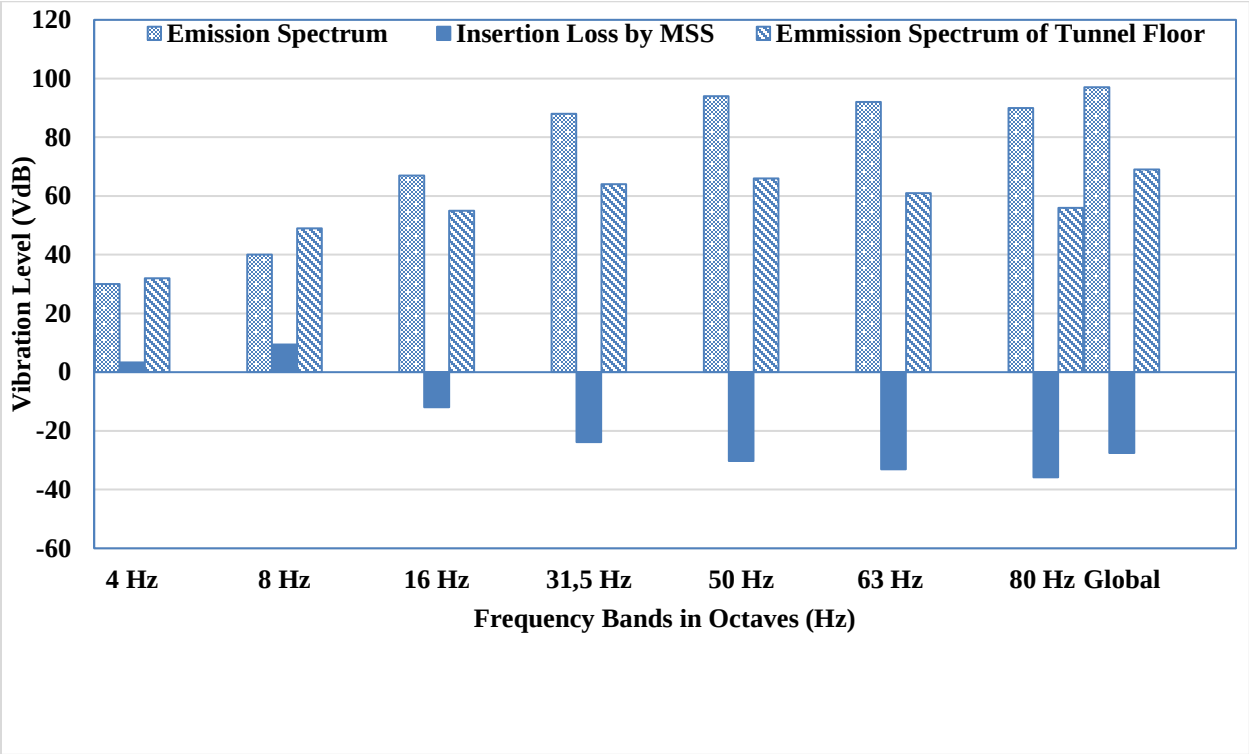

Figure 9. Vibration levels with and without MSS at 30 kmph speed

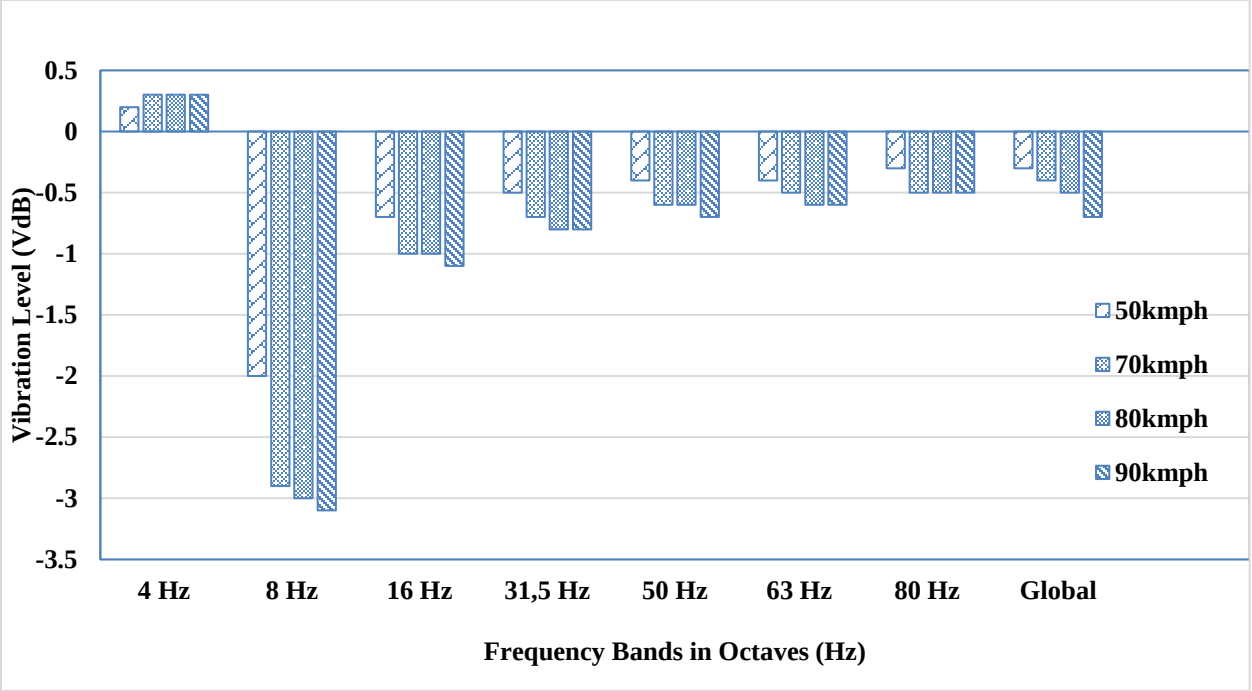

Figure 10. Vibration levels with and without MSS with respect to 30 kmph speed